Weak light emission of soft tissues induced by heating

Weak light emission of soft tissues induced by heating

Antonello E Spinelli[a,*], **Giovanni Durando**[b], **Federico Boschi**[c]
[a]Experimental Imaging Centre, San Raffaele Scientific Institute, Via Olgettina 60, 20182 Milan, Italy
[b]INRIM Ultrasound Laboratory, Strada Delle Cacce 91, 10135 Torino, Italy
[c]Department of Computer Science, University of Verona, Strada Le Grazie 15, 37134 Verona, Italy

Abstract. The main goal of this work is to show that soft tissue interaction with high intensity focused ultrasound (HIFU) or direct heating lead to a weak light emission detectable using a small animal optical imaging system.
Our results shows that the luminescence signal is detectable after 30 minutes from heating resembling the time scale of delayed luminescence.
The imaging of a soft tissue after heating it using an HIFU field shows that the luminescence pattern closely matches the shape of the cone typical of the HIFU beam.
We conclude that heating a soft tissue using two different sources lead to the emission of a weak luminescence signal from the heated region with a decay half life of few minutes (4-6 min). The origin of such light emission needs to be further investigated.

Keywords: optical imaging, weak light emission, heat induced luminescence, high focused ultrasound.

***Corresponding author:** spinelli.antonello@hsr.it

1 Introduction

Optical imaging is a widely used preclinical and clinical tool to investigate *in vivo* different biological processes.[1] In particular bioluminescence imaging (BLI), Cerenkov luminescence imaging (CLI) and radioluminescence imaging (RLI) can be used to detect *in vivo* weak light emission using a small animal optical imaging system. All these imaging approaches do non require the use of any external light source, more precisely bioluminescence light is produced during the enzymatic reaction of luciferase with its substrate, typically firefly and D-luciferin.

Cerenkov luminescence imaging[2] is based on detection of Cerenkov radiation (CR) induced by charged particle (typically beta plus or beta minus particles) as they travel into biological tissue with a velocity greater than the speed of light in the tissue.[3,4]

RLI allows the imaging with optical methods of a large variety of radioisotopes including not just beta but also alpha[5] and gamma emitters.[6–8]

In this work we will investigate another source of light emission in soft tissues caused by heating since in preliminary experiments we measured a weak light emission after treating a slab of chicken breast with high intensity focused ultrasound (HIFU).

HIFU is a non invasive method developed to treat tumors using an ablative approach, and the basic idea is to use HIFU field to increases the temperature in the focal region to ablate the tumor without damaging the surrounding healthy tissues.[9] In this paper we will provide a set of experimental data showing that the interaction with HIFU or direct heating could lead to a weak light emission detectable using a small animal optical imaging system. To the best of our knowledge there are no studies in the literature regarding the use of HIFU, as pure heating source at high temperature (90 °C), connected with luminescence phenomena.

As will be described in the paper the emission of visible light could be interpreted as a mechanism to dissipate energy deposited in the heated tissues. In order to underline the specific source of light emission we called this phenomenon heat induced luminescence (HIL).

2 Material and methods

2.1 High focused ultrasound system

The ultrasound field was generated by a HIFU transducer (Type SU-101; Sonic Concepts, Washington, USA) in Continuous Wave mode at f = 1.1 MHz connected to a power amplifier (Type AR 100A250A; Amplifier Research, Souderton, USA) and a function generator (Type 33250; Agilent, Santa Clara, USA). A mechanical adaptor has been used to connect the 2.5 cm diameter polystyrene tube containing the sample. The HIFU transducer was placed on a 1 cm slab of chicken breast for 1 minute. The ultrasound power was 60 W (Intensity 8×10^3 W/cm^2), Spot size (typically) 1 mm wide $\times$ 3 mm long. The length of the treatment was chosen to increase the tissue

temperature to 90 °C, these setting were find empirically to obtain a detectable emitting thermal lesion (Fig. 1b). The tissue temperature was measured with a FLIR i7 camera (FLIR Systems, Inc. Wilsonville, Oregon, USA), 140x140 pixels, field of view 25° × 25°, accuracy 2%, thermal sensitivity 0.10 °C, minimum focus distance = 0.6 m.

The slab was then cut along the direction of the HIFU field in order to image the light emission induced by the HIFU from the slice surface to the focus region.

2.2 Direct heating source

Direct heating of was obtained using a conventional welding device equipped with a thermometer, the temperature of the tip was set respectively to: 110 °C, 140 °C, 180°C and 250 °C. The tip was placed with a little pressure on top of a 1 cm slab of chicken breast for: 1, 10 and 30 seconds.

Since different pressure and inclination of the welding probe on the sample may limit the reproducibility of the HIL magnitude, measurements were repeated 3 times on different regions of the tissue.

2.3 HIL Images acquisition

Optical images of heated tissues were acquired by using the IVIS Spectrum optical imager (Perkin Elmer, Massachusetts, USA). The IVIS Spectrum is based on a cooled (-90 °C) back-thinned, back-illuminated CCD camera. The CCD has an active array of 1920 x 1920 pixels with a dimension of 13 microns. Images corrected for dark measurements were acquired with Living Image 4.5 (Perkin Elmer).

The acquisition parameters for direct heating were: exposure time = 300 s, aperture f=1, binning B = 16 and Field of View (FoV) = 13.0 cm. Six images were acquired for a total scanning time equal

to 30 minutes.

HIL images when using HIFU heating were acquired using the following setting: exposure time = 120 s, aperture f=1, binning B = 16 and Field of View (FoV) = 13.0 cm. Fifteen images were acquired for a total scanning time equal to 30 minutes. A trade-off was necessary between exposure time and sampling of the HIL, in the case of the HIFU we opted for a better time sampling.

2.4 HIL Image analysis

HIL image analysis was performed by placing region of interests (ROI) over the slab of chicken breast and the total flux *F(t)* (photons/second) within the ROI was measured. Images were analyzed using Living Image 4.5 (Perkin Elmer). The values of the flux measured at different time points were fitted using the following equation:

$$F(t) = (F_0 - B)e^{-kt} + B \tag{1}$$

where the fitting parameters F_0, *B*, and *k* (1/min) are respectively the intercept, the plateau and the decay rate constant of the luminescence signal. The fitting was performed using a non linear least square algorithm implemented in GraphPad Prism, version 5.0.

3 Results

3.1 HIFU heating source

The image in Fig. 1 shows the tissue HIL caused by the HIFU field in a slab of chicken breast. As can be seen there is a good match between the cone heated by the HIFU field and the HIL of the sample.

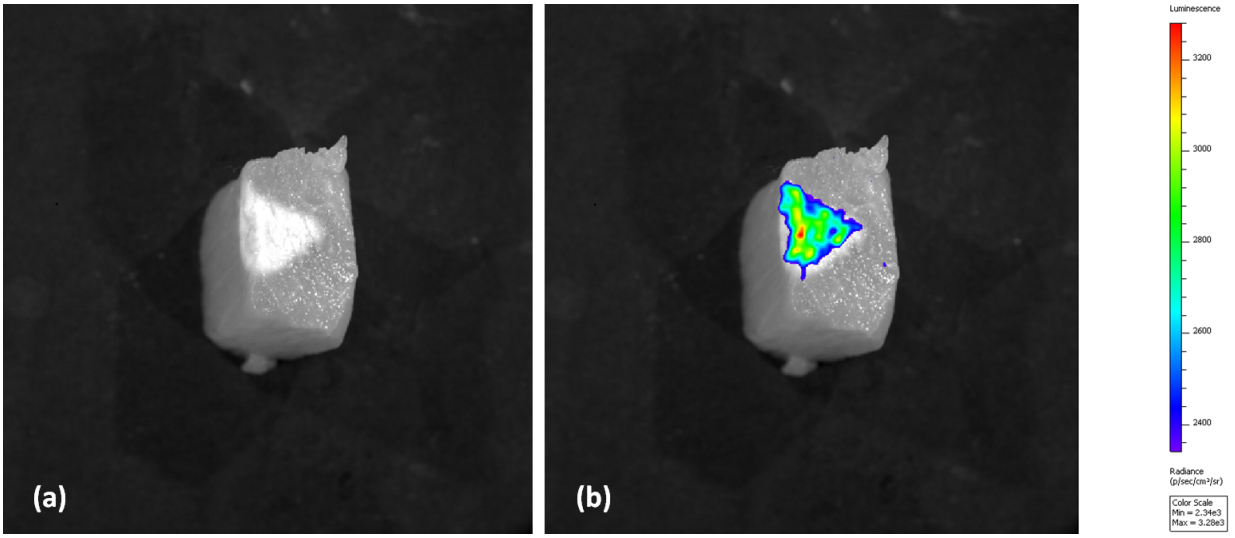

Fig 1 The image shows the tissue HIL by the HIFU field. As can be seen there is a good match between the white cone region heated by the HIFU field (panel a) and the HIL of the sample (panel b).

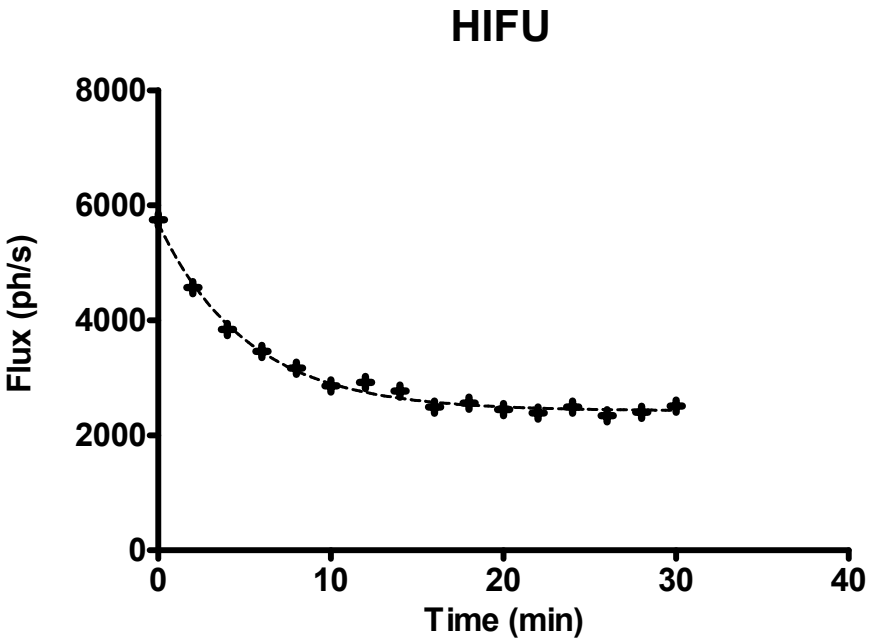

Fig 2 The plot shows the decay of the HIL signal induced by the HIFU field, the half life resulting from the fit was equal to 3.6 min and the R^2 value was equal to 0.99.

The plot in Fig. 2 shows the decay of the HIL signal, the half life resulting from the fit of equation 1 was equal to 3.6 min and the R^2 value was equal to 0.99.

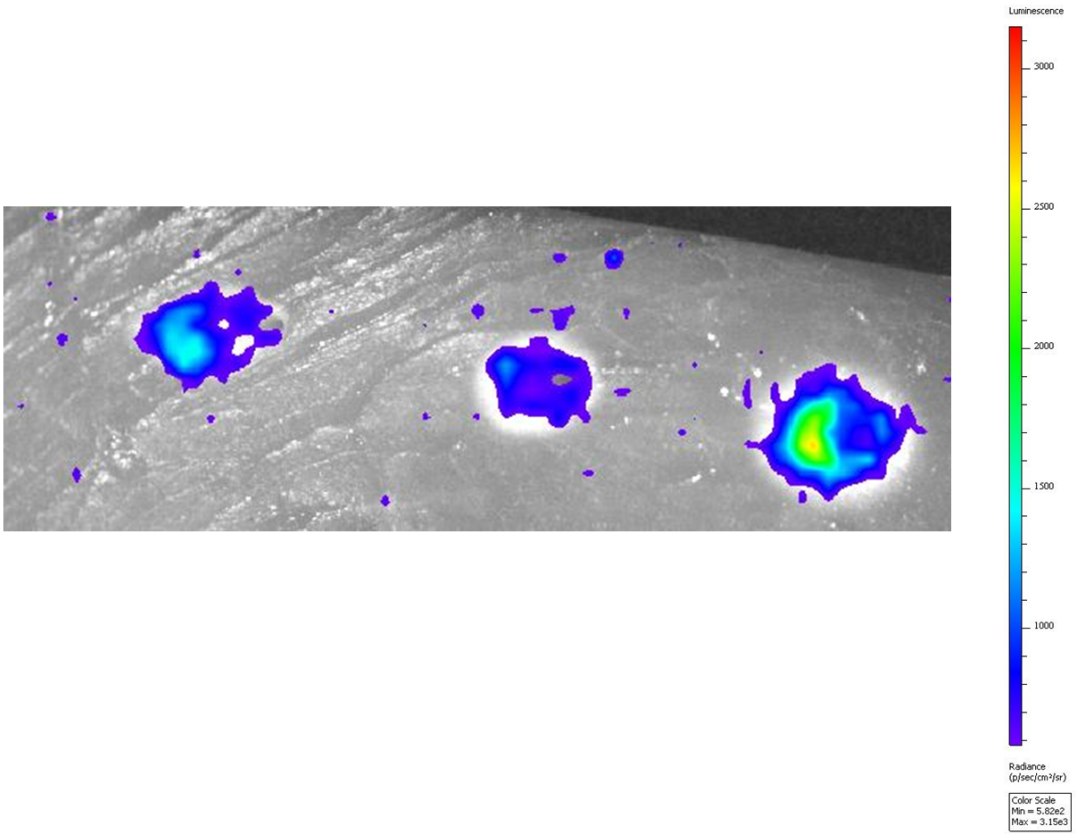

Fig 3 The image shows an example of tissue HIL obtained after 30 min from direct heating using a conventional welding device at a temperature of 140 °C for 1, 10 and 30 seconds (from left to right).

3.2 Direct heating source

The image in Fig. 3 shows the tissue HIL after 30 minutes when heating at a temperature of 140 °C for 1, 10 and 30 seconds a small region (3-5 mm diameter) of the sample. As can be seen HIL is clearly detectable in the tissue in particular when heating for 30 seconds.

Considering the small dimension of the heated region and the delay of 30 minutes between the heating and image acquisition, it is reasonably to consider the whole sample temperature being equal to the environment (about 25°C). This shows that the HIL signal is thus dependent only from the heating time and not from the actual temperature of the spot.

The plots in Fig. 4, Fig. 5 and Fig. 6 show the decay of the HIL signal and the corresponding fitting for the different temperatures 110 °C, 140 °C, 180°C, 250 °C and heating times equal to: 1, 10

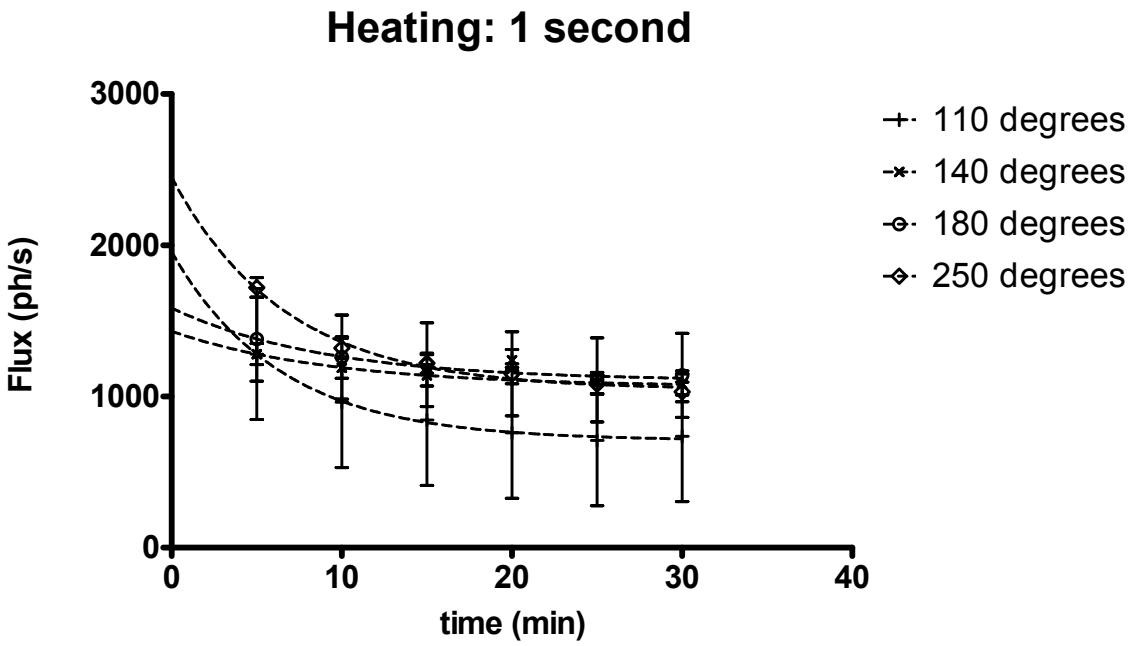

Fig 4 The plot show the decay of the HIL signal and the corresponding fitting (dotted line) for the different temperatures and a heating time equal to 1 second. The heating was obtained with a welding device.

and 30 seconds. The fitting R^2 value is always greater than 0.95 showing a good agreement with equation 1.

The values of the half life obtained from the fit can be found in Fig. 7. Except for one outlier, the range of the half life is between 4 and 6 min. As can be seen by looking at Fig. 7 the value of the half life are mainly dependent from the temperature and not from the heating time. More precisely the half life are similar for the similar temperature even if the heating times are different.

These data are in agreement with the results obtained using HIFU.

4 Discussion and Conclusion

In this work we performed optical imaging of the weak light emission of a soft tissue induced in tissue by heat, in our knowledge a detailed analysis of this phenomenon is not reported in literature. The HIL effect might lead to image artifacts when acquiring CLI or RLI images of specimens from

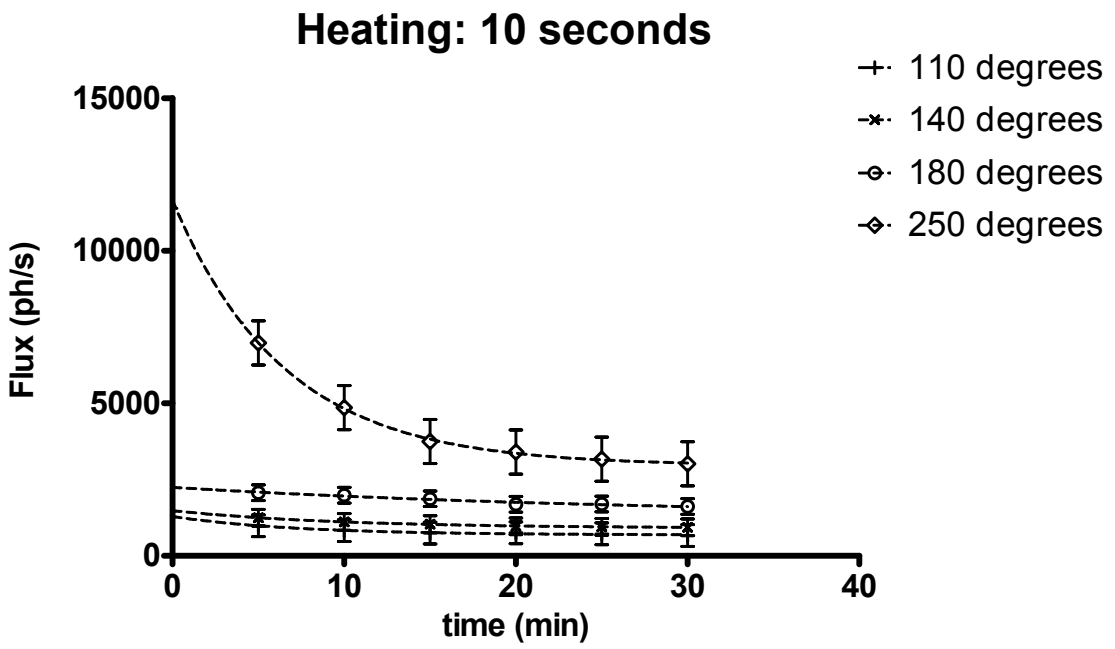

Fig 5 The plot show the decay of the HIL signal and the corresponding fitting (dotted line) for the different temperatures and a heating time equal to 10 seconds. The heating was obtained with a welding device.

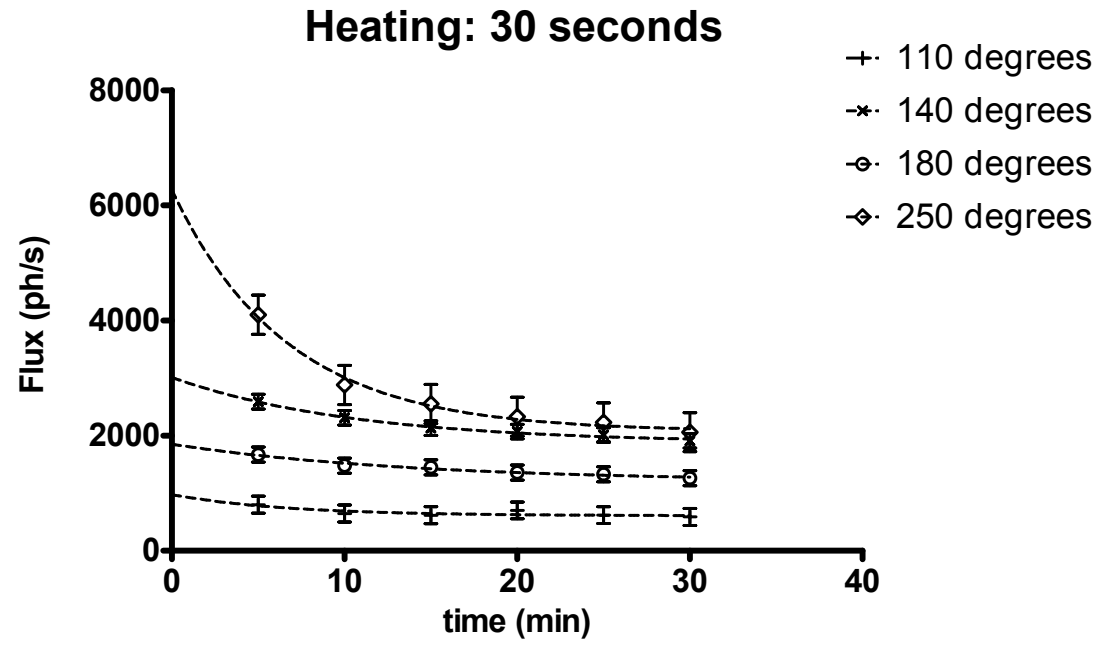

Fig 6 The plot show the decay of the HIL signal and the corresponding fitting (dotted line) for the different temperatures and a heating time equal to 30 seconds.The heating was obtained with a welding device.

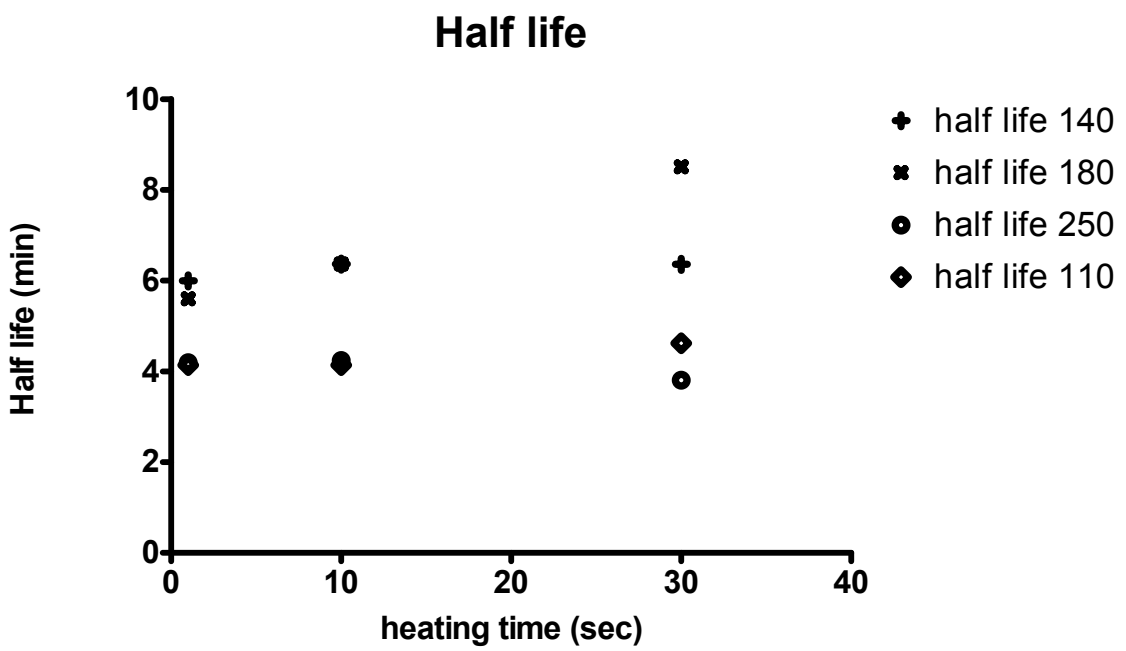

Fig 7 The plot shows the half life obtained from fitting the HIL signal decay using equation 1. Except for two outliers the range of the half life is between 4 and 7 min. The heating was obtained with a welding device.

surgery[10,11] removed using a diathermy device or a laser scalpel.

As shown in Fig. 3 the HIL signal is clearly detectable with respect to background even after 30 minutes from heating the tissue and, thus, this effect resemble the typical time scale of delay luminescence. We imaged for longer time (30 min equal to 5 half life) in order to properly estimate the half life of the HIL signal with respect to the Cerenkov luminescence imaging (CLI). More precisely is well known the half life of CLI is equal to the physical half life of the isotope (e.g. 109 min for ^{18}F or 64.2 h for ^{90}Y) and thus a possible approach to limit the contribution of HLI will be to acquire CLI image at later time e.g. more than 30 minutes where the HIL is about 3% of the initial signal. As mentioned in the result section the interesting aspect is that the decay pattern of the signal is mainly dependent by the initial temperature while is less dependent from the heating time. We can thus claim that the effect is mainly depended on the initial energy deposition only. However it is necessary to point out that a longer heating time causes tissue carbonization and this

might sightly affect the results by reducing the amount of light emitted. We measured the light emission of carbonized regions (using a small region of interest) and we found that the flux was about 5 times lower than in not carbonized areas.

The imaging of a soft tissue after the heating using an HIFU field shows that the luminescence pattern closely matches the shape of the cone typical of an HIFU beam. The decay of the HIL signal is very similar to the decay obtained with the direct heating of the sample using a conventional welding device.

The detection of the HIL will be heavily dependent on the source intensity (e.g. temperature) tissue thickness, optical properties and more importantly on the system minimum detectable radiance.

We conclude that heating a soft tissue using two different sources lead to the emission of a weak luminescence from the heated region with a decay half life of few minutes (4-6 min).The origin of such light emission needs to be further investigated however a possible explanation of the HIL is the light emission due to the generation of reactive oxygen species (ROS) after an heat stress.[12]

Disclosures

The authors have no relevant financial interest to disclose.

References

1 G. D. Luker and K. E. Luker, "Optical imaging: current applications and future directions," *J. Nucl. Med.* **49**, 1–4 (2008).

2 A. Spinelli, D. D'Ambrosio, L. Calderan, *et al.*, "Cerenkov radiation allows in vivo optical imaging of positron emitting radiotracers," **55**(2), 483–495 (2010).

3 A. Spinelli, M. Marengo, R. Calandrino, *et al.*, "Optical imaging of radioisotopes: A novel multimodal approach to molecular imaging," **56**(3), 280–290 (2012).

4 A. E. Spinelli and F. Boschi, "Novel biomedical applications of Cerenkov radiation and radioluminescence imaging," *Phys Med* **31**, 120–129 (2015).

5 F. Boschi, S. Meo, P. Rossi, *et al.*, "Optical imaging of alpha emitters: Simulations, phantom,and in vivo results," **16**(12) (2011).

6 F. Boschi, A. Spinelli, D. D'Ambrosio, *et al.*, "Combined optical and single photon emission imaging: preliminary results.," **54**(23), L57–62 (2009).

7 A. Spinelli, S. Meo, R. Calandrino, *et al.*, "Optical imaging of tc-99m-based tracers: In vitro and in vivo results," **16**(11) (2011).

8 F. Boschi, M. Pagliazzi, B. Rossi, *et al.*, "Small-animal radionuclide luminescence imaging of thyroid and salivary glands with tc99m-pertechnetate," **18**(7) (2013).

9 M. C. L. Peek and M. Douek, "Ablative techniques for the treatment of benign and malignant breast tumours," *J Ther Ultrasound* **5**, 18 (2017).

10 A. E. Spinelli, M. P. Schiariti, C. M. Grana, *et al.*, "Cerenkov and radioluminescence imaging of brain tumor specimens during neurosurgery," *J Biomed Opt* **21**, 50502 (2016).

11 M. R. Grootendorst, M. Cariati, S. E. Pinder, *et al.*, "Intraoperative Assessment of Tumor Resection Margins in Breast-Conserving Surgery Using (18)F-FDG Cerenkov Luminescence Imaging: A First-in-Human Feasibility Study," *J. Nucl. Med.* **58**, 891–898 (2017).

12 K. Kobayashi, H. Okabe, S. Kawano, *et al.*, "Biophoton emission induced by heat shock," *PLoS ONE* **29**(8), e105700 (2014).

Antonello E Spinelli received his PhD in medical physics from the Institute of Cancer Research, University of London, UK, in 2004, and the medical physics expert degree from the University of Bologna, in 2009. He is the small animal optical imaging research coordinator of the San Raffaele

Scientific Institute, Milan, Italy. His main research areas are in vivo optical imaging, Cerenkov and radioluminescence imaging, and preclinical CT imaging.

Giovanni Durando received his PhD in metrology from Politecnico di Torino, IT, in 2003. In May 2009, he accepted a permanent position as a physicist at INRIM (Istituto Nazionale di Ricerca Metrologica) in the Metrology for the Quality of Life Department. He is an active member of IEC-TC 87 (Ultrasonics) and is a delegate for CCAUV (Consultative Committee for Acoustic, Ultrasound and Vibration). His experimental activity is focused on acoustics, ultrasound, and metrology.

Federico Boschi received his PhD from the University of Verona in 2008 and is now a researcher at the Optical Imaging Laboratory, University of Verona. Before his PhD, he was involved in different research activities in astrophysics and he switched to preclinical imaging working with small animal MR and optical imaging in 2004. His main research areas are Cerenkov and radioluminescence imaging, in vivo optical imaging using nanoparticles, and small animal magnetic resonance imaging.

List of Figures

List of Tables